Disilane Chromophores

International Edition: DOI: 10.1002/anie.201509380
German Edition: DOI: 10.1002/ange.201509380

Bright Solid-State Emission of Disilane-Bridged Donor–Acceptor–Donor and Acceptor–Donor–Acceptor Chromophores

Masaki Shimada, Mizuho Tsuchiya, Ryota Sakamoto, Yoshinori Yamanoi, Eiji Nishibori, Kunihisa Sugimoto, and Hiroshi Nishihara**

Abstract: *The development of disilane-bridged donor–acceptor–donor (D-Si-Si-A-Si-Si-D) and acceptor–donor–acceptor (A-Si-Si-D-Si-Si-A) compounds is described. Both types of compound showed strong emission (λ_{em} = ca. 500 and ca. 400 nm, respectively) in the solid state with high quantum yields (Φ: up to 0.85). Compound* ***4*** *exhibited aggregation-induced emission enhancement in solution. X-ray diffraction revealed that the crystal structures of* ***2****,* ***4****, and* ***12*** *had no intermolecular π–π interactions to suppress the nonradiative transition in the solid state.*

In recent years, π-conjugated triads with electron-donating (D) and electron-accepting (A) groups (D-π-A-π-D or A-π-D-π-A compounds) have received attention because of their potential uses as photonic and electronic materials.[1] The most important feature of these molecules is intramolecular charge-transfer (ICT). It leads to photoabsorption, strong emission, electroluminescence, and nonlinear optical properties, making them promising candidates for OLEDs[2] and two-photon fluorescent probes.[3] However, emissions from π-conjugated systems can be lost through quenching owing to π–π stacking in the aggregated state (aggregation-caused quenching).[4] Moreover, intermolecular π–π stacking also leads to low solubility in solvents. Given that the strong intermolecular interactions of aggregates often limit the emission performance and uses of highly soluble, donor–acceptor-based molecules displaying solid-state fluorescent molecules are desired.

Oligosilane derivatives display light emission and electron transport properties both in solution and in the solid state.[5] Efficient solid emission and high solubility result from the suppression of intermolecular interactions owing to the tetrahedral structure and large atomic radius of the silicon. We previously reported aryl oligosilanes that displayed strong florescence in the solid state.[6] However, no oligosilane-bridged D-A-D or A-D-A compound has yet been reported. Herein, we report the photophysical properties of disilane-bridged D-A-D molecules (D-Si-Si-A-Si-Si-D) and A-D-A molecules (A-Si-Si-D-Si-Si-A). The chemical structures of six D-A-D compounds **1**–**6** and six A-D-A compounds **7**–**12** prepared in this work are shown in Figure 1. These compounds displayed interesting photophysical properties, particularly high quantum yields in the solid state.

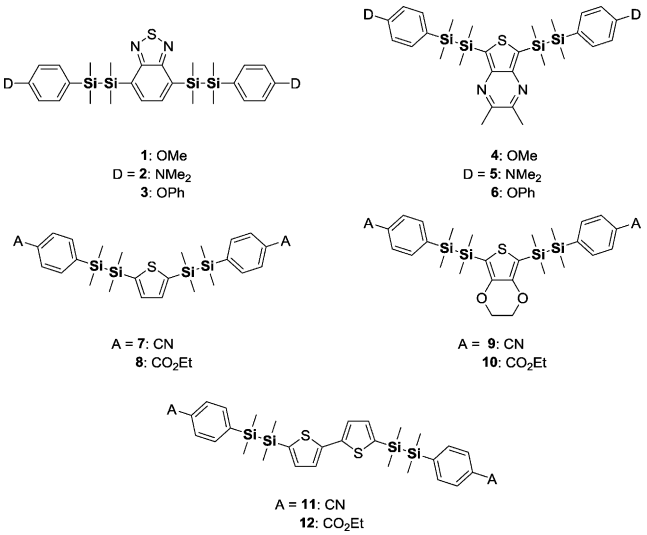

Figure 1. Chemical structures of disilane-bridged D–A–D derivatives **1**—**6** and A–D–A derivatives **7**—**12**.

Compounds **1**–**12** studied in this work are designed to clarify the relationship between their structure and optical properties. D-A-D molecules (**1**–**6**) were readily synthesized by the Pd-catalyzed coupling reaction of electron-accepting 4,7-diiodo-2,1,3-benzothiadiadiazole or 5,7-diiodo-2,3-dimethylthieno[3,4-*b*]pyrazine moieties with hydrosilanes derived from the corresponding donor moieties. A-D-A molecules (**7**–**12**) were prepared by the same coupling reaction of iodoarenes bearing ester or cyano groups at their *p*-positions with 2,5-bis(1,1,2,2-tetramethyldisilanyl) thiophene, 2,5-bis(1,1,2,2-tetramethyldisilanyl)-3,4-ethylenedioxythiophene (EDOT), or 5,5′-bis(1,1,2,2-tetramethyldisilanyl)-2,2′-bithiophene. All of the compounds were characterized by ^{1}H NMR and ^{13}C NMR spectroscopy and high-resolution mass spectrometry or elementary analysis.

[*] M. Shimada, M. Tsuchiya, Dr. R. Sakamoto, Dr. Y. Yamanoi, Prof. H. Nishihara
Department of Chemistry, School of Science, The University of Tokyo
7-3-1 Hongo, Bunkyo-ku, Tokyo 113-0033 (Japan)
E-mail: yamanoi@chem.s.u-tokyo.ac.jp
nisihara@chem.s.u-tokyo.ac.jp
Prof. E. Nishibori
Division of Physics, Faculty of Pure and Applied Sciences, Tsukuba Research Center for Interdisciplinary Materials Science (TIMS) & Center for Integrated Research in Fundamental Science and Engineering (CiRfSE), University of Tsukuba
1-1-1 Tennodai, Tsukuba, Ibaraki 305–8571 (Japan)
Dr. K. Sugimoto
Japan Synchrotron Radiation Research Institute (JASRI)
1-1-1 Koto, Sayo-cho, Sayo-gun, Hyogo 679–5198 (Japan)

Supporting information for this article is available on the WWW under http://dx.doi.org/10.1002/anie.201509380.

Table 1: Detailed optical properties of **1**–**12**.

	In CH_2Cl_2[a]					Solid state[b]			
Compound	λ_{abs} [nm]	ε [$\times 10^3$ M^{-1}cm^{-1}]	λ_{em} [nm]	Φ[c]	τ [ns][d]	λ_{ex}[e] [nm]	λ_{em} [nm]	Φ[c]	τ [ns][d]
1	357	6.86	–[f]	–[f]	–[f]	370	486	0.85	7.8[g]
2	357	6.35	630	<0.01	2.7[g]	370, 421[h]	500	0.34	4.7[i]
3	353	7.54	489	<0.01	–[f]	371	490	0.26	1.9 (50%) 4.1 (50%)[g]
4	383	5.10	500	0.04	1.1[g]	442	491	0.44	10.2[i]
5	384	4.83	500	0.01	0.63 (95%) 2.7 (5%)[g]	450	504	0.16	3.6 (39%) 10.4 (61%)[j]
6	380	4.62	497	0.06	1.5[g]	–[k]	–[k]	–[k]	–[k]
7	272	27.0	428, 460	0.18	1.9[l]	342	391	0.11	0.7[m]
8	272	30.8	434, 467	0.32	1.9[l]	287	385	0.44	0.68[l]
9	278	27.5	436, 461	0.04	1.5[l]	–[k]	–[k]	–[k]	–[k]
10	280	28.4	461	0.09	0.29 (23%) 2.2 (77%)[l]	329	405	0.32	0.85 (99%) 12.1 (1%)[m]
11	332	19.3	398	0.40	0.95[g]	365	410	0.66	1.7[g]
12	334	24.0	399	0.34	0.97[g]	370	411	0.77	2.3[g]

[a] Measured in anhydrous degassed CH_2Cl_2. [b] Optical properties of compounds **1**, **2**, **4**, **8**, **11**, and **12** were in microcrystalline powder and those of compounds **3**, **5**, **7**, and **10** were in amorphous powder. [c] Absolute quantum yields were determined by an integrating sphere system. [d] Fluorescence lifetimes were detected at the maximum fluorescence wavelengths. [e] Excitation wavelengths in the solid state determined by excitation spectra. [f] Under detection limit. [g] Excited at 365 nm. [h] Shoulder peak. [i] Excited at 405 nm. [j] Excited at 465 nm. [k] Oil products. [l] Excited at 280 nm. [m] Excited at 340 nm.

The absorption and photoluminescence of **1**–**12** in dichloromethane and in the solid state are given in Table 1 and the Supporting Information, Figures S2–S13. The lowest-energy absorption bands of the D-A-D molecules were located at 360–385 nm, caused by the ICT transitions between the peripheral donor groups and the acceptor core. The absorption bands of the A-D-A molecules containing thiophene or EDOT (**7**–**10**) were in the UV region at 270–280 nm, whereas those of the molecules containing the 2,2′-bithiophene moiety (**11**, **12**) were located at around 330 nm. The absorption wavelength of A-D-A molecules reflects the σ–π conjugated system of the donor moiety.

The photoluminescence spectra of the D-A-D molecules in CH_2Cl_2 mostly showed broad bands at around 500 nm; however, the band for **2** is located at 630 nm. Emission spectra of **2** and **5** in acetone displayed dual emission at around 500 nm and over 600 nm. The latter peak and 630 nm of **2** in CH_2Cl_2 are assignable to twisted ICT emission due to twisting dimethylamino group in the excited state (Supporting Information, Figures S14 and S15 and Tables S9 and 10).[7] The emission spectra of the A-D-A molecules with thiophene or EDOT as the central aryl (**7**–**10**) showed emissions around 450 nm and large Stokes shifts between the absorption and emission maxima. In comparison, the A-D-A molecules with 2,2′-bithiophene moieties (**11**, **12**) displayed narrower emission bands at shorter wavelengths (around 400 nm). Compounds **7**–**10** displayed solvatochromism, indicating that the dipole moment was larger in the excited state than in the ground state.

Fluorescence quantum yields (Φ) are also listed in Table 1. The low quantum yields observed in dichloromethane mainly depended on the central aryl. The D-A-D molecules **1**–**3** showed emission quantum yields ($\Phi < 0.02$) lower than those of **4**–**6** (Φ: 0.02–0.08). The A-D-A molecules were ranked in order of increasing quantum yield by their constituent moieties as 2,2′-bithiophene (**11**, **12**), thiophene (**7**, **8**), and EDOT (**9**, **10**). The lower quantum yield in solution of **9** and **10** was caused by the nonradiative relaxation channels induced by the flexibility of the ethylenedioxy moieties.[8]

Fluorescence in the solid state was either blue–green (D-A-D) or blue (A-D-A), with an unstructured emission profile showing maxima around 500 (**1**–**5**) or 400 nm (**7**, **8**, **10**–**12**). All but one (**7**) showed much higher quantum yields in the solid state than in solution. In the solid state, compound **1** exhibited a maximum emission band at 486 nm (blue emission) with a high quantum yield ($\Phi = 0.85$), and **11** and **12** also displayed strong emission around 410 nm with high quantum yields ($\Phi = 0.66$ and 0.77, respectively).

We investigated the aggregation-induced emission (AIE) of **4** by the THF/water method, as shown in Figure 2 and the Supporting Information, Figure S17.[9] The addition of water to a THF solution of **4** initially decreased the original weak photoluminescence. However, when water comprised over 70% of the total solvent volume fraction ($f_w = 70\%$), the fluorescence intensity dramatically increased, and the photoluminescence intensity of **4** in 99% water was more than three times that in 100% THF. This suggests that the strong emission was induced by aggregation, which could suppress the nonradiative relaxation channels such as vibration and rotation. Note that the emission and excitation spectra did not depend on the THF/water ratio (Supporting Information, Figure S17), and the concentration dependence was not observed (Supporting Information, Table S12). Furthermore, compound **6** also displayed AIE like **4** (Supporting Information, Figures S18–S21).

To examine the photoemission dynamics, the fluorescence rate constants (k_f) and nonradiative rate constants (k_{nr}) of selected compounds were determined (Supporting Information, Table S13) by using the fluorescence lifetimes (τ) and

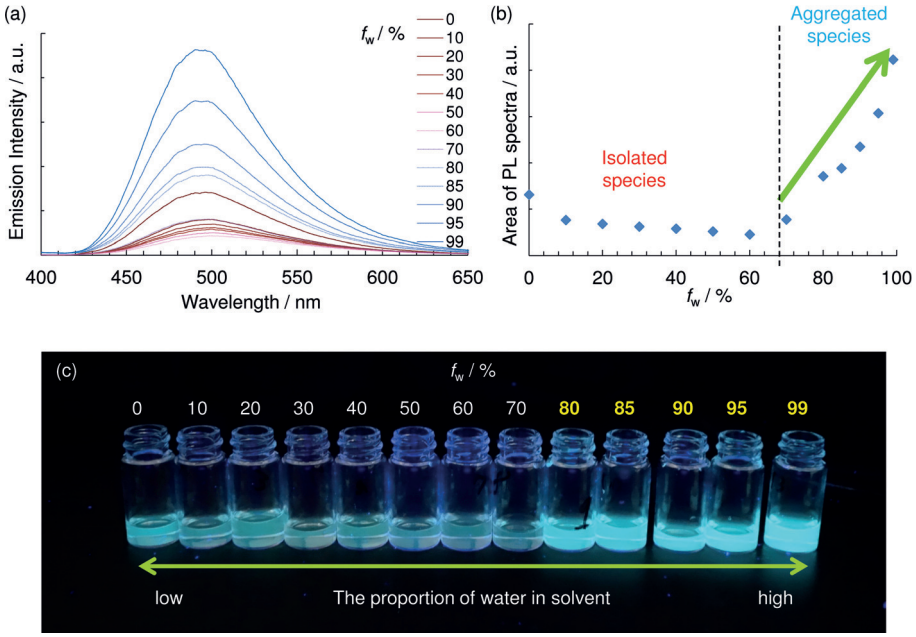

Figure 2. Measurement of the aggregation effect of **4**. f_w is expressed as a percent of water in the total solvent volume; $f_w = V_{water}/(V_{THF} + V_{water})$, where V is volume. a) Fluorescence spectra in various THF/water mixtures. b) Plot of fluorescence intensity (area) vs. f_w. c) Photographs of the photoluminescence in various THF/water mixtures under UV irradiation (365 nm).

quantum yields. The fluorescence rate constants of **4** and **12** showed little difference between solution and the solid state, whereas the nonradiative rate constant in solution was much larger than that in the solid state. This dramatic difference insists that nonradiative relaxation in the solid state was reduced compared to that in solution. Furthermore, the solvent effect of compound **4** on optical properties was investigated. The quantum yield decreased and k_{nr} increased as the polarity of the solvent was increased, which can be ascribed to a photoelectron transfer (PET) process (Supporting Information, Tables S11, S14).[10] These results suggest that the higher Φ values in the solid state is due to the suppression of nonradiative relaxation and the reduction of PET effect.

Single-crystal X-ray diffraction results for **2**, **4**, **8**, and **12** indicate their molecular packing structures (Figures 3; Supporting Information, Figure S1).[11] The molecular structure of **2** appears almost straight (Figure 3a), and its crystal packing is grid-like structure without π–π stacking (Figure 3b). The structure of **4** displayed a *syn* and twisted form (Figure 3c). Its crystal structure (Figure 3d) has the terminal donor aromatic ring (T2) and the central acceptor aromatic ring (C) located nearly parallel in the *anti*-position, and the other terminal aromatic ring (T1) is twisted relative to the central aromatic ring (C). There is no π–π stacking in the crystal, which is due to the twisted molecular structure. A-D-A molecule **12** (Figure 3e) shows an *anti*-formed straight structure, which is similar to that of compound **8** (Supporting Information, Figures S1a). The crystal packing of both compounds (Supporting Information, Figures S1b and 3f) shows no intermolecular π–π interactions. Overall, both the D-A-D and the A-D-A molecules displayed strong fluorescence in the solid state without quenching owing to the effective suppression of intermolecular interactions as well as the suppression of nonradiative relaxation channels and PET effect.[4d]

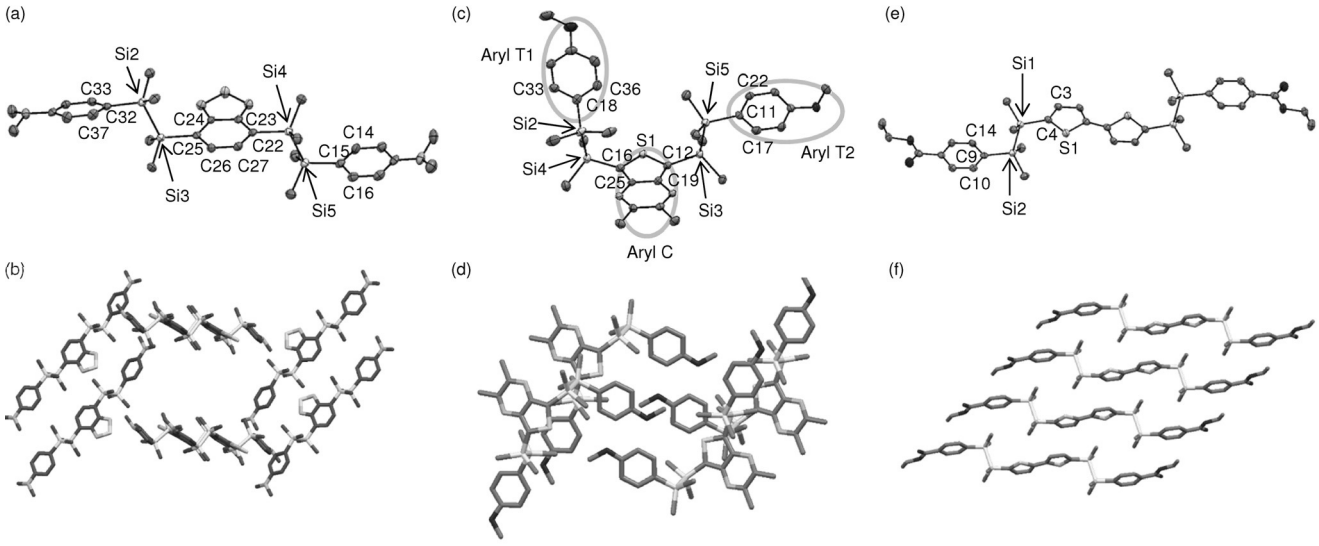

Figure 3. a), c), e) ORTEP drawings (ellipsoids set at 50% probability) and b), d), f) packing structures of a), b) **2**, c), d) **4**, and e), f) **12**. Hydrogen atoms are omitted for clarity.

To investigate the effects of donor and acceptor aryls on the optical properties, we calculated the molecular orbitals and excited states with density functional theory (DFT) and time-dependent DFT (TD-DFT). The electron density of the HOMO of **1** was spread over the donor aryls, and the LUMO was mainly localized on the acceptor aryls. Although the electron density of the LUMO of **4** was localized on the acceptor groups, similar to **1**, its HOMO was mainly localized on the thiophene and silicon moieties (Supporting Information, Figure S22). Note that the frontier molecular orbitals of *anti*-form **4** in solution did not greatly differ from those of the *syn*-form in the solid state. The TD-DFT calculation showed that the lowest energy absorption band of **1** represented the HOMO→LUMO transition (Supporting Information, Table S15), which was assigned to ICT absorption. The lowest energy absorption band of **4** was also the HOMO→LUMO transition (Supporting Information, Table S16), and was assigned to a combination of ICT and π–π* excitation. The fluorescence of **1** was assigned to only ICT emission, via a charge separation state, whereas that of **4** was assigned to ICT and π–π* emission.

The electron density of the HOMOs of A-D-A molecules **8** and **10** was mainly localized on the central aromatic and silicon moieties, and the LUMO was localized on the acceptor aromatic ring. In contrast, both the HOMO and LUMO of **12** were localized on the 2,2′-bithiophene and silyl groups (Supporting Information, Figure S23). TD-DFT calculations showed the lowest energy absorption band of **8** to represent the HOMO→LUMO transition assignable to ICT, whereas that of **12** represents the HOMO→LUMO π–π* excitation (Supporting Information, Tables S17–S19). Therefore, the fluorescence of **8** and **10** can be assigned to ICT emission, whereas that of **12** can be assigned to the π*→π emission. This appears to account for **7**–**10** displaying larger Stokes shifts than **11**–**12**.

In conclusion, we systematically synthesized a series of disilane-bridged D-A-D and A-D-A molecules **1**–**12**. They displayed broad UV/Vis absorption bands assigned to ICT or π–π* transition and excitation, which led to strong fluorescence in the solid state (Φ: up to 0.85). Compound **4** displayed aggregation-induced emission in THF/water solution. These disilane-bridged triads, which display high fluorescence efficiencies in the solid state achieved here, are desirable for various applications such as organic electroluminescence devices.

Acknowledgements

We thank Dr. Aiko Kamitsubo, the Elemental Analysis Center of The University of Tokyo, for the elemental analysis measurements. The work was financially supported by CREST, JST for H.N., PRESTO, JST for R.S., Tokyo Kasei Chemical Promotion foundation, and Grant-in-Aids for Scientific Research (C) (No. 15K05604), Scientific Research on Innovative Areas "Molecular Architectonics: Orchestration of Single Molecules for Novel Functions" (area 2509, Nos. 26110506 and 26110506) from the Ministry of Education, Culture, Sports, Science, and Technology, Japan. The synchrotron radiation experiments were performed at the SPring-8 with the approval of the Japan Synchrotron Radiation Research Institute (JASRI) (No. 2015A1374).

Keywords: aggregation · disilanes · fluorescence · silicon · solid-state structures

How to cite: *Angew. Chem. Int. Ed.* **2016**, *55*, 3022–3026
Angew. Chem. **2016**, *128*, 3074–3078

[1] a) J. Zhang, W. Chen, J. A. Rojas, V. E. Jucov, V. E. Timofeeva, C. T. Parker, S. Barlow, R. S. Marder, *J. Am. Chem. Soc.* **2013**, *135*, 16376–16379; b) M. H. Kim, R. B. Cho, *Chem. Commun.* **2009**, 153–164; c) L. Chen, L, Wang, X. Jing, *J. Mater. Chem.* **2011**, *21*, 10265–10267; d) D. Liang, S. Tang, J. Liu, J. Liu, L. Kang, *J. Mol. Struct. THEOCHEM* **2009**, *908*, 102–106.

[2] a) F. B. Dias, K. N. Bourdakos, V. Jankus, K. C. Moss, K. T. Kamtekar, V. Bhalla, J. Santos, M. R. Bryce, A. P. Monkman, *Adv. Mater.* **2013**, *25*, 3707–3714; b) L. Duan, J. Qiao, Y. Sun, Y. Qiu, *Adv. Mater.* **2011**, *23*, 1137–1144; c) Y. Zhu, A. P. Kulkarni, S. A. Jenekhe, *Chem. Mater.* **2005**, *17*, 5225–5227; d) B. A. D. Neto, A. S. Lopes, G. Ebeling, R. S. Goncalves, V. E. U. Costa, F. H. Quina, J. Dupont, *Tetrahedron* **2005**, *61*, 10975–10982.

[3] a) S. Yao, H.-Y. Ahn, X. Wang, J. Fu, E. W. Van Stryland, D. J. Hagan, K. D. Belfield, *J. Org. Chem.* **2010**, *75*, 3965–3974; b) S. Ellinger, K. R. Graham, P. Shi, R. T. Farley, T. T. Steckler, R. N. Brookins, P. Taranekar, J. Mei, L. A. Padilha, T. R. Ensley, H. Hu, S. Webster, D. J. Hagan, E. W. Van Stryland, K. S. Schanze, J. R. Reynolds, *Chem. Mater.* **2011**, *23*, 3805–3817; c) K. Susumu, J. A. N. Fisher, J. Zheng, D. N. Beratan, A. G. Yodh, M. J. Therien, *J. Phys. Chem. A* **2011**, *115*, 5525–5539; d) S. Kato, T. Matsumoto, T. Ishi-i, T. Thiemann, M. Shigeiwa, H. Gorohmaru, S. Maeda, Y. Yamashita, S. Mataka, *Chem. Commun.* **2004**, 2342–2343.

[4] a) G. S. Beddard, G. Porter, *Nature* **1976**, *260*, 366–367; b) Y. Hong, J. W. Y. Lam, B. Z. Tang, *Chem. Commun.* **2009**, 4332–4353; c) R. Jakubiak, C. J. Collison, W. C. Wan, L. J. Rothberg, B. R. Hsieh, *J. Phys. Chem. A* **1999**, *103*, 2394–2398; d) Y. Kubota, Y. Ozaki, K. Funabiki, M. Matsui, *J. Org. Chem.* **2013**, *78*, 7058–7067; e) Y. Ooyama, T. Okamoto, T. Yamaguchi, T. Suzuki, A. Hayashi, K. Yoshida, *Chem. Eur. J.* **2006**, *12*, 7827–7838.

[5] a) K. Takahashi, Y. Nishimura, T. Arai, S. Yagai, A. Kitamura, T. Karatsu, *J. Photochem. Photobiol. A* **2011**, *218*, 204–212; b) S. Kyushin, K. Yoshimura, K. Sato, H. Matsumoto, *Chem. Lett.* **2009**, *38*, 324–325; c) M. Shimizu, H. Tatsumi, K. Mochida, K. Oda, T. Hiyama, *Chem. Asian J.* **2008**, *3*, 1238–1247; d) H.-S. Oh, I. Imae, Y. Kawakami, S. S. S. Raj, T. Yamane, *J. Organomet. Chem.* **2003**, *685*, 35–43; e) D.-D. H. Yang, N.-C. C. Yang, I. M. Steele, H. Liu, Y.-Z. Ma, G. R. Fleming, *J. Am. Chem. Soc.* **2003**, *125*, 5107–5110; f) M. Shimizu, K. Oda, Y. Bando, T. Hiyama, *Chem. Lett.* **2006**, *35*, 1022–1023; g) H. Tsuji, Y. Shibano, T. Takahashi, M. Kumada, K. Tamao, *Bull. Chem. Soc. Jpn.* **2005**, *78*, 1334–1344; h) Y. Shibano, M. Sasaki, Y. Kawanishi, Y. Araki, H. Tsuji, O. Ito, K. Tamao, *Chem. Lett.* **2007**, *36*, 1112–1113; i) M. Sasaki, Y. Shibano, H. Tsuji, Y. Araki, K. Tamao, O. Ito, *J. Phys. Chem. A* **2007**, *111*, 2973–2979.

[6] a) A. Lesbani, H. Kondo, J.-i. Sato, Y. Yamanoi, H. Nishihara, *Chem. Commun.* **2010**, *46*, 7784–7786; b) H. Inubushi, Y. Hattori, Y. Yamanoi, H. Nishihara, *J. Org. Chem.* **2014**, *79*, 2974–2979; c) M. Shimada, Y. Yamanoi, T. Matsushita, T. Kondo, E. Nishibori, A. Hatakeyama, K. Sugimoto, H. Nishihara, *J. Am. Chem. Soc.* **2015**, *137*, 1024–1027.

[7] C. Cao, X. Liu, Q. Qiao, M. Zhao, W. Yin, D. Mao, H. Zhang, Z. Xu, *Chem. Commun.* **2014**, *50*, 15811–15814.

[8] M. Belletête, S. Beaupré, J. Bouchard, P. Blondin, M. Leclerc, G. Durocher, *J. Phys. Chem. B* **2000**, *104*, 9118 – 9125.
[9] a) Y. Hong, J. W. Y. Lam, B. Z. Tang, *Chem. Soc. Rev.* **2011**, *40*, 5361 – 5388; b) X. Y. Shen, Y. J. Wang, E. Zhao, W. Z. Yuan, Y. Liu, P. Lu, A. Qin, Y. Ma, J. Z. Sun, B. Z. Tang, *J. Phys. Chem. C* **2013**, *117*, 7334 – 7347.
[10] a) M.-Y. Yeh, H.-C. Lin, T.-S. Lim, S.-L. Lee, C.-H. Chen, W. Fann, T.-Y. Luh, *Macromolecules* **2007**, *40*, 9238 – 9243; b) C.-H. Chen, W.-H. Chen, Y.-H. Liu, T.-S. Lim, T.-Y. Luh, *Chem. Eur. J.* **2012**, *18*, 347 – 354; c) J. Ohshita, F. Kaneko, D. Tanaka, Y. Ooyama, *Asian J. Org. Chem.* **2014**, *3*, 170 – 175.
[11] CCDC 1425714 (**2**), 1425711 (**4**), 1425712 (**8**) and 1425713 (**12**) contain the supplementary crystallographic data for this paper. These data are provided free of charge by The Cambridge Crystallographic Data Centre.

Received: October 7, 2015
Revised: December 9, 2015
Published online: January 28, 2016

